

2-2-2024

## Analytical solution of deformation of underlying shield tunnel caused by foundation pit excavation and dewatering

Ling-xiao GUAN

State Key Laboratory of Performance Monitoring Protecting of Rail Transit Infrastructure, East China Jiaotong University, Nanchang, Jiangxi 330013, China; Engineering Research & Development Centre for Underground Technology of Jiangxi Province, East China Jiaotong University, Nanchang, Jiangxi 330013, China; Jiangxi Key Laboratory of Infrastructure Safety Control in Geotechnical Engineering, East China Jiaotong University, Nanchang, Jiangxi 330013, China, glx1392@163.com

Chang-jie XU

State Key Laboratory of Performance Monitoring Protecting of Rail Transit Infrastructure, East China Jiaotong University, Nanchang, Jiangxi 330013, China; Engineering Research & Development Centre for Underground Technology of Jiangxi Province, East China Jiaotong University, Nanchang, Jiangxi 330013, China; Jiangxi Key Laboratory of Infrastructure Safety Control in Geotechnical Engineering, East China Jiaotong University, Nanchang, Jiangxi 330013, China, xucj@zju.edu.cn

Xue-peng WANG

State Key Laboratory of Performance Monitoring Protecting of Rail Transit Infrastructure, East China Jiaotong University, Nanchang, Jiangxi 330013, China; Engineering Research & Development Centre for Underground Technology of Jiangxi Province, East China Jiaotong University, Nanchang, Jiangxi 330013, China; Jiangxi Key Laboratory of Infrastructure Safety Control in Geotechnical Engineering, East China Jiaotong University, Nanchang, Jiangxi 330013, China  
Follow this and additional works at: <https://rocksoilmech.researchcommons.org/journal>



Part of the [Geotechnical Engineering Commons](#)

Xue-qin XIA

State Key Laboratory of Performance Monitoring Protecting of Rail Transit Infrastructure, East China Jiaotong University, Nanchang, Jiangxi 330013, China; Engineering Research & Development Centre for Underground Technology of Jiangxi Province, East China Jiaotong University, Nanchang, Jiangxi 330013, China; Ling-xiao GUAN, Chang-jie XU, Chang-jie WANG, Xue-peng WANG, Xue-qin XIA, and KE Wen-hai (2024). Analytical solution of deformation of underlying shield tunnel caused by foundation pit excavation and dewatering, "Rock and Soil Mechanics: Vol. 44: Iss. 11, Article 7.

DOI: 10.16285/j.rsm.2022.6961

Available at: <https://rocksoilmech.researchcommons.org/journal/vol44/iss11/7>

See next page for additional authors

This Article is brought to you for free and open access by Rock and Soil Mechanics. It has been accepted for inclusion in Rock and Soil Mechanics by an authorized editor of Rock and Soil Mechanics.

---

# Analytical solution of deformation of underlying shield tunnel caused by foundation pit excavation and dewatering

## Abstract

The foundation pit excavation and dewatering break the equilibrium stress field of the surrounding soil layer and negatively affect the underlying shield tunnel. The analytical solution of the longitudinal deformation of the underlying tunnel caused by foundation pit excavation and dewatering is proposed using a two-stage analysis method. In the first stage, Mindlin elastic solution and effective stress principle are used to calculate the additional stress caused by excavation and dewatering. In the second stage, the shield tunnel is treated as a Timoshenko beam resting on the Pasternak foundation to simulate the interaction between the tunnel and soil. The analytical solution of the longitudinal tunnel deformation is derived from the superposition method. By comparing with the monitoring data of engineering examples, the correctness of the proposed method is verified, and the influence of the excavation length, width, depth, tunnel burial depth, dropdown, and relative position of the foundation pit on the longitudinal displacement of the tunnel is further analyzed. The results show that with the increase of excavation length, width, and depth, the maximum uplift of the tunnel increases. The tunnel deformation decreases with the increase in tunnel burial depth. With the increase of the dropdown, the uplift decreases, and the settlement value increases. With the increased distance between the tunnel axis and the foundation pit center, there are a decreasing area of the uplift, an increasing area of the settlement, and a decreasing area of settlement.

## Keywords

foundation pit excavation, foundation pit dewatering, underlying shield tunnel, shear deformation, Timoshenko beam, Pasternak foundation

## Authors

Ling-xiao GUAN, Chang-jie XU, Xue-peng WANG, Xue-qin XIA, and Wen-hai KE

# Analytical solution of deformation of underlying shield tunnel caused by foundation pit excavation and dewatering

GUAN Ling-xiao<sup>1, 2, 3</sup>, XU Chang-jie<sup>1, 2, 3</sup>, WANG Xue-peng<sup>1, 2, 3</sup>, XIA Xue-qin<sup>1, 2, 3</sup>, KE Wen-hai<sup>1, 2, 3</sup>

1. State Key Laboratory of Performance Monitoring Protecting of Rail Transit Infrastructure, East China Jiaotong University, Nanchang, Jiangxi 330013, China

2. Engineering Research & Development Centre for Underground Technology of Jiangxi Province, East China Jiaotong University, Nanchang, Jiangxi 330013, China

3. Jiangxi Key Laboratory of Infrastructure Safety Control in Geotechnical Engineering, East China Jiaotong University, Nanchang, Jiangxi 330013, China

**Abstract:** The foundation pit excavation and dewatering break the equilibrium stress field of the surrounding soil layer and negatively affect the underlying shield tunnel. The analytical solution of the longitudinal deformation of the underlying tunnel caused by foundation pit excavation and dewatering is proposed using a two-stage analysis method. In the first stage, Mindlin elastic solution and effective stress principle are used to calculate the additional stress caused by excavation and dewatering. In the second stage, the shield tunnel is treated as a Timoshenko beam resting on the Pasternak foundation to simulate the interaction between the tunnel and soil. The analytical solution of the longitudinal tunnel deformation is derived from the superposition method. By comparing with the monitoring data of engineering examples, the correctness of the proposed method is verified, and the influence of the excavation length, width, depth, tunnel burial depth, dropdown, and relative position of the foundation pit on the longitudinal displacement of the tunnel is further analyzed. The results show that with the increase of excavation length, width, and depth, the maximum uplift of the tunnel increases. The tunnel deformation decreases with the increase in tunnel burial depth. With the increase of the dropdown, the uplift decreases, and the settlement value increases. With the increased distance between the tunnel axis and the foundation pit center, there are a decreasing area of the uplift, an increasing area of the settlement, and a decreasing area of settlement.

**Keywords:** foundation pit excavation; foundation pit dewatering; underlying shield tunnel; shear deformation; Timoshenko beam; Pasternak foundation

## 1 Introduction

Foundation pit engineering and subway construction are effective means of underground space development. However, with the development of underground space construction, foundation pit projects adjacent to existing subway tunnels have become commonplace<sup>[1–3]</sup>. Foundation pit excavation and dewatering break the equilibrium stress field of the soil layer, which induces deformation of the surrounding soil and underground structures<sup>[4–6]</sup>. In particular, underground subway tunnels are significantly affected by foundation pit excavation and dewatering, such as a foundation pit engineering in Nanning<sup>[7]</sup> caused a significant mutation uplift. A foundation pit project in Shanghai still caused 14.7 mm uplift deformation in multiple prevention and control measures<sup>[8]</sup>. Failure to prevent and control the effects of foundation pit construction may cause serious accidents such as tunnel segment cracking and water seepage and affect its service performance<sup>[9]</sup>. Therefore, predicting and assessing the stress and deformation of the underlying shield tunnel caused by excavation and dewatering of the foundation pit is an urgent issue.

Currently, numerous scholars have conducted research on the impact of foundation pit excavation and dewatering on adjacent tunnels through various methods. For example, He et al.<sup>[10]</sup> utilized FLAC<sup>3D</sup> to study the deformation patterns of surrounding tunnels

during foundation pit excavation and dewatering. Zhang et al.<sup>[11]</sup> established finite element models based on actual engineering and studied the impact patterns of different dewatering schemes on the deformation of surrounding tunnels during foundation pit excavation. However, there is currently limited theoretical research on the longitudinal deformation of nearby tunnels caused by the combined effects of foundation pit excavation and dewatering. Ou et al.<sup>[12]</sup> used Euler-Bernoulli beam theory to simulate the stress and deformation of the tunnel, considering the influence of unloading at the pit bottom and dewatering on the underlying shield tunnel. The research results indicate that the impact of foundation pit dewatering on the underlying shield tunnel should not be ignored. Xu et al.<sup>[13]</sup>, based on a two-stage approach and incorporating the principle of effective stress in soil and the Pasternak foundation model, used Euler-Bernoulli beams to simulate pipelines and derived analytical solutions for the deformation of nearby pipelines caused by single-well dewatering. Additionally, Liang et al.<sup>[14]</sup> simplified shield tunnels as Euler-Bernoulli beams to study the impact of foundation pit excavation on tunnels.

The above-mentioned literature considers the tunnel as a Euler-Bernoulli beam. However, since the Euler-Bernoulli beam only accounts for the flexural stiffness of the tunnel, treating the shear stiffness as

Received: 16 December 2022

Accepted: 11 April 2023

This work was supported by the National Natural Science Foundation of China (52238009), the Natural Science Foundation of Jiangxi Province (20224BAB214068) and the Innovation Fund for Postgraduate of Jiangxi Province (YC2021-S433).

First author: GUAN Ling-xiao, male, born in 1996, PhD candidate, focusing on soil-structure interaction. E-mail: glx1392@163.com

Corresponding author: XU Chang-jie, male, born in 1972, PhD, Professor, PhD supervisor, research interests: soil dynamics, foundation pit engineering, and tunnel engineering. E-mail: xucj@zju.edu.cn

infinite, it cannot take into account the shear deformation generated when the tunnel is subjected to forces. However, the structure of shield tunnels consists of multiple segmented ring-shaped sections, which have relatively low shear stiffness. Using Euler-Bernoulli beams to simulate shield tunnels can lead to a certain degree of error<sup>[15]</sup>. Therefore, in recent years, some scholars have used Timoshenko beams, which consider shear deformation, to simulate tunnels in other research areas<sup>[16–17]</sup>. Zhang et al.<sup>[17]</sup> used Timoshenko beams to simulate tunnels and studied the longitudinal displacement of existing tunnels caused by shield tunneling underneath. Liang et al.<sup>[18]</sup> proposed analytical solutions for tunnel deformation caused by foundation pit excavation based on Timoshenko beams. Research indicates that using Timoshenko beams to simulate shield tunnels has certain advantages<sup>[16–18]</sup>. Furthermore, current theoretical research seldom comprehensively considers the combined effects of foundation pit excavation and dewatering on the underlying shield tunnel. However, dewatering, as an essential step in foundation pit engineering, leads to an increase in the effective stress of the soil below the original water level, resulting in adverse effects on existing tunnels below<sup>[19–20]</sup>. It is also one of the primary reasons for long-term tunnel settlement<sup>[1]</sup>. As a result, the impact of foundation pit dewatering should not be overlooked in relevant theoretical research.

In conclusion, to address the shortcomings in existing theoretical research, this study builds upon previous work and conducts a study on the deformation of the underlying shield tunnel caused by the combined effects of foundation pit excavation and dewatering using a two-stage approach. In the first stage, the Mindlin elastic solution<sup>[21]</sup> is used to calculate the additional stresses caused by excavation at the pit bottom and the surrounding walls. Based on the principle of effective stress and the Dupuit assumption, additional stresses induced by dewatering on the nearby tunnel are calculated. In the second stage, the total stresses caused by excavation and dewatering are applied to the underlying shield tunnel. The shield tunnel is treated as a Timoshenko beam capable of considering shear deformation, lying on a Pasternak foundation. Displacement control equations for the tunnel are established, and analytical solutions for the longitudinal deformation of the tunnel are derived using the superposition method. Subsequently, the proposed method in this study is compared with actual engineering monitoring data, confirming the accuracy of this approach. Furthermore, the study conducts an in-depth investigation into the effects of excavation length, depth, and tunnel burial depth on the longitudinal deformation of the tunnel.

## 2 Additional stress caused by foundation pit excavation and dewatering

The construction of foundation pit engineering inevitably involves two construction phases: earthwork

excavation and groundwater dewatering. When there is an existing subway tunnel beneath the foundation pit, the unloading effect caused by earthwork excavation and the increase in effective stress in the soil due to dewatering result in additional stresses on the underlying shield tunnel. To simplify the calculation of the additional stresses on the tunnel, an approach in present study assumes that the soil involved in the calculations is considered as isotropic elastic material.

### 2.1 Additional stress caused by foundation pit excavation

As shown in Fig.1, when the existing subway tunnel is located beneath the foundation pit, the additional stress at the tunnel axial position, induced by the unloading from foundation pit excavation, is caused by the unloading at the pit bottom and the four sidewalls.

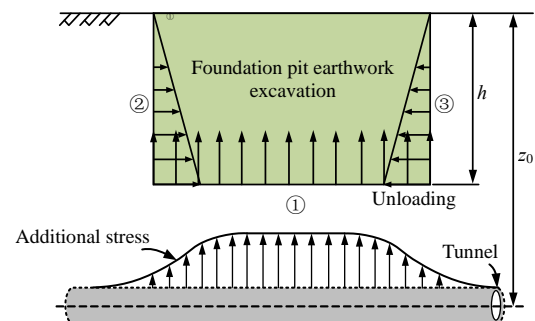


Fig. 1 Simplified calculation model diagram

The additional stress caused by unloading at the pit bottom, denoted as '①', can be obtained using the Mindlin elastic solution<sup>[21]</sup>:

$$q_1(x) = \int_{-B/2}^{B/2} \int_{-L/2}^{L/2} \frac{p_i d\xi d\eta}{8\pi(1-\nu)} \left[ -\frac{(1-2\nu)(z_0-h)}{R_1^3} + \frac{(1-2\nu)(z_0-h)}{R_2^3} - \frac{3(z_0-h)^3}{R_1^5} - \frac{3(3-4\nu)z_0(z_0+h)^2 - 3h(z_0+h)(5z_0-h)}{R_2^5} - \frac{30hz_0(z_0+h)^3}{R_2^7} \right] \quad (1)$$

where  $q_1$  is the additional stress caused by unloading ① at the pit bottom;  $B$ ,  $L$ , and  $h$  represent the foundation pit excavation width, length, and depth;  $p$  is the total unloading due to the earthwork excavation,

$p_i = \sum_{i=1}^n \gamma_i H_i$ ,  $\gamma_i$  and  $H_i$  represent the actual density

and layer thickness of  $i$ -th soil layer;  $\nu$  is Poisson's ratio;  $\eta$  and  $\xi$  represent the two axes of the coordinate system established with the foundation pit center as the origin, as shown in Fig.2;  $z_0$  is the burial depth of tunnel axis; and  $R_1$  and  $R_2$  represent the position relationship functions between points on the tunnel axis and the center of the foundation pit. These functions are determined by the relative positioning of the tunnel and the foundation pit.

$$\left. \begin{aligned} R_1 &= \sqrt{(X - \xi)^2 + (Y - \eta)^2 + (z_0 - h)^2} \\ R_2 &= \sqrt{(X - \xi)^2 + (Y - \eta)^2 + (z_0 + h)^2} \end{aligned} \right\} \quad (2)$$

where  $X$  and  $Y$  represent the abscissa and ordinate of a specific point on the tunnel in the coordinate system  $\xi O \eta$ . As shown in Fig.2, the  $\xi O \eta$  coordinate system is established with the center of the foundation pit as the origin  $O$ , parallel to the length direction and width direction of the foundation pit as  $\xi$  and  $\eta$  axes. Furthermore, a  $xO'y$  coordinate system is established with a point along the tunnel axis as the coordinate origin " $O'$ ", the tunnel axis as the  $x$ -axis, and the direction perpendicular to it as the  $y$ -axis. Based on the positional relationship between the two coordinate systems, the coordinate transformation formula can be derived as follows:

$$\left. \begin{aligned} X &= y \sin \alpha + x \cos \alpha + d \cos \beta \\ Y &= y \cos \alpha - x \sin \alpha + d \sin \beta \end{aligned} \right\} \quad (3)$$

where  $\alpha$  represents the angle between the  $\xi$  and  $x$  axis and  $\beta$  represents the angle between  $\xi$  and the line segment  $OO'$ ; and  $d$  is the length of line segment  $OO'$ .

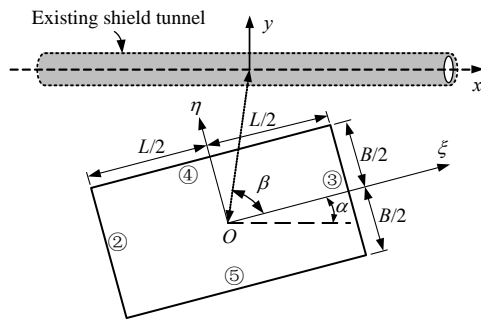


Fig. 2 Plane position relation between the foundation pit and the underlying tunnel

According to the Mindlin elastic solution<sup>[21]</sup>, the additional stress caused by the unloading of the foundation pit sidewall "②" can be calculated as follows:

$$\begin{aligned} q_2(x) &= \int_{-B/2}^{B/2} \int_0^h \frac{K_0 \gamma z x d\xi dz}{8\pi(1-\nu)} \left[ -\frac{(1-2\nu)}{T_1^3} + \right. \\ &\quad \left. \frac{(1-2\nu)}{T_2^3} + \frac{3(z_0 - z)^2}{T_1^5} + \right. \\ &\quad \left. \frac{3(3-4\nu)z_0(z_0 + z)^2 - 6z^2 - 6z(1-2\nu)(z_0 + z)}{T_2^5} - \right. \\ &\quad \left. \frac{30zz_0(z_0 + z)^2}{T_2^7} \right] \end{aligned} \quad (4)$$

where  $K_0$  is static earth pressure coefficient, which can be determined through laboratory or in-situ static lateral pressure tests. In the absence of test data, it can also be estimated using empirical formulas. Sandy soil:

$K_0 = 1 - \sin \phi$ ; clay soil:  $K_0 = 0.95 - \sin \phi$ ; over-consolidated clay soil:  $K_0 = \text{OCR}(1 - \sin \phi)$ ,  $\phi$  is effective internal friction angle, OCR denotes over-consolidation ratio; and  $T_1$  and  $T_2$  refer to position relationship functions between points along the tunnel axis and the foundation pit sidewall. These functions are determined by the relative positioning of the foundation pit and the tunnel:

$$\left. \begin{aligned} T_1 &= \sqrt{\left(X - \frac{L}{2}\right)^2 + (Y - \eta)^2 + (z_0 - z)^2} \\ T_2 &= \sqrt{\left(X - \frac{L}{2}\right)^2 + (Y - \eta)^2 + (z_0 + z)^2} \end{aligned} \right\} \quad (5)$$

Similarly, the additional stresses  $q_3(x)$ ,  $q_4(x)$ ,  $q_5(x)$  caused by the unloading effect of side walls ③, ④, and ⑤ on the tunnel can be obtained. The total additional stress at the tunnel axis caused by foundation pit excavation can be calculated using the superposition principle.

## 2.2 Additional stress caused by foundation excavation dewatering

The literature [22] has found that using the virtual large diameter well to calculate the deformation of pipelines caused by foundation pit dewatering is more accurate. Therefore, in this study, the foundation pit is treated as a large dewatering well, assuming that there is a certain hydraulic connection between the inside and outside of the foundation pit, and the groundwater level on both sides of the retaining structure is the same. Based on the Dupuit assumption, the formula for calculating the groundwater level curve around the foundation pit caused by dewatering is as follows:

$$h(r) = \sqrt{H_0^2 - (H_0^2 - H_t^2) \frac{\ln \frac{R + R_0}{R_0}}{\ln \frac{R + R_0}{R_0}}} \quad (6)$$

where  $r = \sqrt{x^2 + d^2}$ ,  $r$  is the horizontal distance between the point on the tunnel axis and the well center;  $H_0$  represents the initial water level height of phreatic aquifer;  $H_t$  represents the water level height inside the pit after dewatering;  $R_0 = \sqrt{BL/\pi}$  is the radius of the dewatering well;  $R = 2s_w \sqrt{kH_0}$  is the influence radius of dewatering<sup>[23]</sup>;  $s_w = H_0 - H_t$  is the drawdown. As shown in Fig.3, within the dewatering radius, a drop in water level leads to a decrease in pore water pressure in the soil, subsequently causing an increase in effective stress. Based on the principle of effective stress, effective stress increment can be derived:

$$\Delta \sigma = \sigma_t - \sigma_0 = (H_0 - h)(\gamma - \gamma_s + \gamma_w) \quad (7)$$

where  $\Delta \sigma$  is the increment in effective stress;  $\sigma_0$  and  $\sigma_t$  are the effective stresses within the soil before and after dewatering;  $\gamma$ ,  $\gamma_s$ , and  $\gamma_w$  are the natural unit weight, saturated unit weight of soil, and the unit weight of water. It should be noted that, after

foundation pit excavation, this study does not consider the increment in effective stress caused by the dewatering of the excavated soil. The variation in effective stress of the pit is related to the soil layers beneath the water level, but this study does not delve into a detailed discussion of this aspect. Therefore, the additional stress caused by foundation pit dewatering on the underlying shield tunnel can be expressed as

$$\Delta\sigma(x) = \begin{cases} H_0 - \sqrt{\left(H_0^2 - H_t^2\right) \frac{\ln \frac{R+R_0}{R_0}}{\ln \frac{R+R_0}{R_0}}} \\ (\gamma - \gamma_s + \gamma_w), x \geq \sqrt{R_0^2 - d^2} \\ h_1(\gamma - \gamma_s + \gamma_w), x < \sqrt{R_0^2 - d^2} \end{cases} \quad (8)$$

where  $h_1$  is the distance from the water level inside the pit to the pit bottom.

In summary, it is assumed that the additional stresses due to foundation pit unloading and dewatering are independent of each other, the additional stress at the tunnel axis induced by foundation pit excavation and dewatering is as follows:

$$q(x) = \sum_{i=1}^5 q_i(x) + \Delta\sigma(x) \quad (9)$$

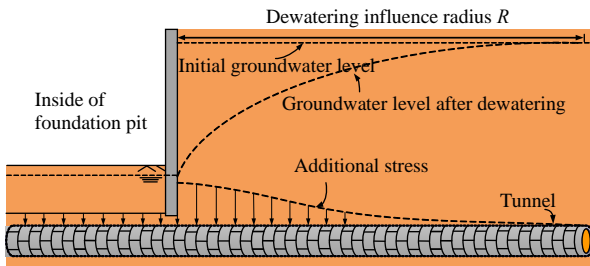


Fig. 3 Additional stress caused by dewatering

### 3 Tunnel governing equations based on Timoshenko beam theory

The longitudinal deformation resulting from shield tunneling consists of both bending deformation and shear deformation<sup>[24–25]</sup>. When using the traditional Euler-Bernoulli beam model to simulate shield tunnels, the shear deformation of the tunnel is neglected. Because shield tunnels are assembled using ring-shaped segments, using the Euler-Bernoulli beam model to simulate the deformation under stress will result in some degree of error. Therefore, in this study, the tunnel is considered as an infinitely long Timoshenko beam on a Pasternak foundation, as shown in Fig.4. The Pasternak foundation model, based on the Winkler foundation model, takes into account the continuity of soil deformation. It consists of soil springs and shear layers that experience shear deformation only, making it superior to the Winkler foundation<sup>[26]</sup>. Timoshenko beam considers the shear deformation of the tunnel when longitudinal deforma-

tion occurs under stress. After deformation, the beam section perpendicular to the neutral axis is no longer perpendicular to the neutral axis due to shear deformation, but forms an angle with the normal direction of the neutral axis, as shown in Fig. 5. The model in this paper assumes the coordination of deformation between the tunnel and the soil during tunnel–soil interaction caused by pit excavation and precipitation.

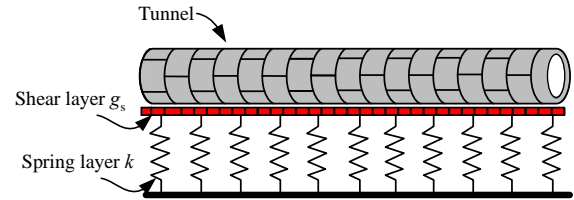


Fig. 4 Pasternak-Timoshenko foundation beam model

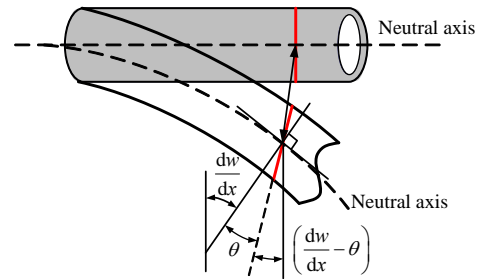


Fig. 5 Timoshenko beam deformation mode

According to Timoshenko beam deformation theory, the relationships between tunnel bending moment  $M$ , shear force  $Q$ , and displacement  $w$  are as follows:

$$Q = (\kappa GA) \left[ \frac{dw(x)}{dx} - \theta \right] \quad (10)$$

$$M = -E_t I_t \frac{d\theta}{dx} \quad (11)$$

where  $\kappa$  is the equivalent section factor, and since the tunnel has a circular cross-section, it is taken as 0.5;  $G = E_t / 2(1 + \nu_t)$  is the shear modulus;  $\nu_t$  is Poisson's ratio;  $A$  represents the cross-sectional area of the tunnel;  $E_t$  is the elastic modulus;  $I_t$  is the moment of inertia.

According to the equilibrium differential equation, we have

$$p(x) D dx - q(x) D dx - dQ = 0 \quad (12)$$

$$\frac{p(x) D}{2} dx^2 + Q dx - \frac{q(x) D}{2} dx^2 - dM = 0 \quad (13)$$

where  $q(x)$  is the additional loading caused by excavation and dewatering;  $D$  represents the diameter of the tunnel.  $p(x)$  is the foundation reaction force. According to the Pasternak foundation model,  $p(x)$  can be expressed as follows:



$$p(x) = kw(x) - g_s \frac{d^2 w(x)}{dx^2} \quad (14)$$

where  $k$  and  $g_s$  represent the elastic and shear coefficient, which can be calculated using the following equations [27–28]:

$$k = \frac{1.3E_s}{D(1-\nu^2)} \left( \frac{E_s D^4}{E_t I_t} \right)^{1/12} \quad (15)$$

$$g_s = \frac{E_s t}{6(1+\nu)} \quad (16)$$

where  $E_s$  is the elastic modulus;  $t$  is the shear layer thickness, and it is taken as  $t=2.5D$  for calculation based on reference [29].

By combining Eqs. (10) to (14) and simplifying, the governing equation for the displacement  $w(x)$  of the tunnel can be obtained as follows:

$$\frac{d^4 w(x)}{dx^4} - \gamma \frac{d^2 w(x)}{dx^2} + \lambda^4 w(x) = \left[ \frac{\kappa GA q(x)}{\kappa GA + g_s D} - \frac{E_t I_t}{\kappa GA + g_s D} \frac{d^2 q(x)}{dx^2} \right] \frac{D}{E_t I_t} \quad (17)$$

where

$$\gamma = \frac{kDE_t I_t + g_s D \kappa GA}{(\kappa GA + g_s D) E_t I_t}, \quad \lambda = \sqrt[4]{\frac{kD \kappa GA}{(\kappa GA + g_s D) E_t I_t}} \quad (18)$$

## 4 Solutions to governing equations

Equation (17) is relatively complex and difficult to solve directly. So first seek its general solution. Let  $q(x)=0$ , the general solution of Eq.(17) can be obtained:

$$w(x) = e^{\alpha_1 x} [A_1 \cos(\beta_1 x) + A_2 \sin(\beta_1 x)] + e^{-\alpha_1 x} [A_3 \cos(\beta_1 x) + A_4 \sin(\beta_1 x)] \quad (19)$$

where  $A_1$ ,  $A_2$ ,  $A_3$ , and  $A_4$  are the coefficients to be determined  $\alpha_1 = \sqrt{\lambda^2/2 + \gamma/4}$ ;  $\beta_1 = \sqrt{\lambda^2/2 - \gamma/4}$ .

When a concentrated load  $P$  acts on the tunnel at  $x=0$ , as  $x$  approaches infinity ( $x \rightarrow \infty$ ), the tunnel displacement is  $w=0$ . Additionally, at  $x=0$ , the tunnel cross-section remains perpendicular to the neutral axis after loading, without rotation because it is located directly under the concentrated force. Therefore, the tunnel still satisfies a zero-angle of rotation and shear force equilibrium at this point. Hence, the boundary conditions for the tunnel at this moment are:

$$\left. \begin{aligned} w(\pm\infty) &= 0 \\ \frac{dw(x)}{dx} \Big|_{x=0} &= 0 \\ E_t I_t \frac{d^3 w(x)}{dx^3} \Big|_{x=0} &= PD/2 \end{aligned} \right\} \quad (20)$$

Substituting Eq.(20) into Eq.(19), the displacement equation for the tunnel under the concentrated load  $P$  can be determined as follows:

$$w(x) = \frac{PDe^{-\alpha_1 x} (\beta_1 \cos \beta_1 x + \alpha_1 \sin \beta_1 x)}{4E_t I_t \alpha_1 \beta_1 (\alpha_1^2 + \beta_1^2)} \quad (21)$$

According to Eq.(17), the right side terms of the equation is regarded as  $Q(x)$ , and the concentrated load  $P(\xi)$  on any point  $\xi$  on the tunnel is:

$$P(\xi) = Q(\xi) d\xi = \left[ \frac{\kappa GA}{\kappa GA + g_s D} q(\xi) - \frac{E_t I_t}{\kappa GA + g_s D} \frac{d^2 q(x)}{dx^2} \right]_{x=\xi} d\xi \quad (22)$$

Substituting this concentrated load into Eq.(21) yields the vertical displacement  $dw(x)$  of the tunnel:

$$dw(x) = \frac{Q(\xi)De^{-\alpha_1 |x-\xi|}}{4E_t I_t \alpha_1 \beta_1 (\alpha_1^2 + \beta_1^2)} [\beta_1 \cos(\beta_1 |x-\xi|) + \alpha_1 \sin(\beta_1 |x-\xi|)] d\xi \quad (23)$$

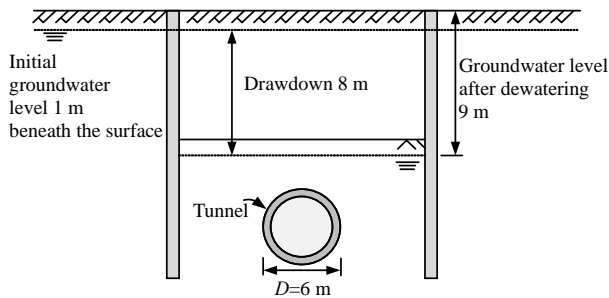
By integrating Eq. (23) within the influence range of foundation pit dewatering, we can obtain the vertical displacement of the tunnel caused by foundation pit excavation and dewatering:

$$w(x) = \int_{-\sqrt{R^2-d^2}}^{\sqrt{R^2-d^2}} dw(x) \quad (24)$$

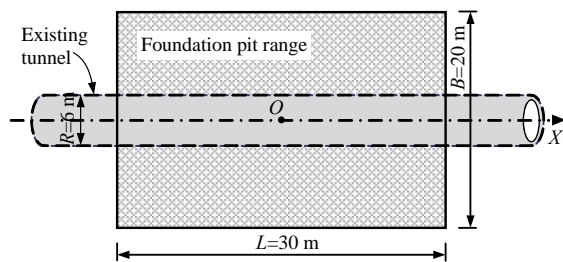
## 5 Example verification

To validate the accuracy of the method presented in this paper, it was verified based on the deformation monitoring data of an existing shield tunnel caused by dewatering and excavation of the foundation pit<sup>[30]</sup>. The foundation pit excavation dimensions are 30 m × 20 m × 8 m (length × width × depth). Due to the combined effect of dewatering and excavation, the construction of this foundation pit will inevitably lead to deformation of the underlying shield tunnel. The existing shield tunnel is located directly beneath the foundation pit ( $d=0$ ) and is longitudinally parallel to the foundation pit. The relative positions of the tunnel and the foundation pit are shown in Fig.6. The depth of tunnel axis  $z_0 = 14$  m, the radius  $D = 6$  m, and the wall thickness is 0.3 m. The segments are made of C50 concrete, so its elastic modulus is taken as  $E_t = 34.5$  GPa, the Poisson's ratio  $\nu_t = 0.3$ . According to the method in literature [31–32], the bending stiffness and shear modulus of the tunnel can be calculated to be  $7.548 \times 10^5$  MN · m<sup>2</sup> and  $2.212 \times 10^3$  MPa. The tunnel is located in gravelly clay soil layer, and its elastic modulus  $E_s = 18$  MPa, permeability coefficient  $k_t = 1$  m/d, Poisson's ratio  $\nu = 0.3$ , natural unit weight and saturated unit weight are  $\gamma = 19.9$  kN/m<sup>2</sup> and  $\gamma_s = 20.4$  kN/m<sup>2</sup>. The parameter values involved in Eqs. (22) to (24) in this case are shown in Table 1. The initial water level in this project is 1 meter below the

ground, and as the foundation pit construction begins, the water level gradually drops to 1 meter below the pit bottom. Therefore, the drawdown is  $s_w = 8$  m.



(a) Section graph

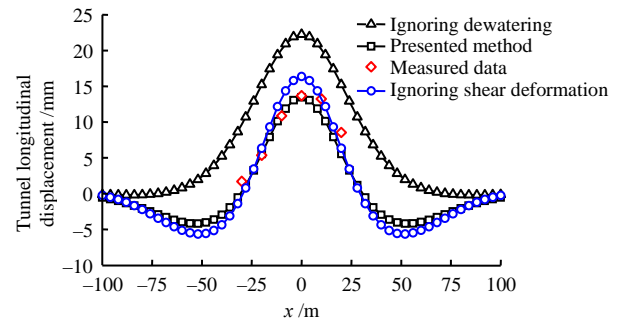


(b) Planar graph

**Fig. 6 Schematic diagram of working conditions****Table 1 Parameters used in calculation**

$\alpha_1$	$E_p I_t$	$D$	$k$	$\beta_1$	$\kappa GA$	$R$	$g_s$
$/m^{-1}$	$/(MN \cdot m^2)$	$/m$	$/(kN \cdot m^{-3})$	$/m^{-1}$	$/kN$	$/m$	$/(kN \cdot m^{-1})$
0.058	$7.548 \times 10^5$	6	$3.21 \times 10^3$	0.04	$5.94 \times 10^6$	77.82	$3.46 \times 10^4$

Figure 7 presents a comparison between the results by method proposed in this paper, the results without considering dewatering effects, the results without considering tunnel shear deformation, and the actual engineering measurements. As seen from Fig.7, the tunnel deformation predicted by considering the combined effects of foundation pit excavation and dewatering is closer to the actual measured values. The maximum measured deformation of the tunnel is 13.68 mm. The maximum deformation calculated using the method proposed in this study, the one when ignoring the dewatering effect, and the one when ignoring tunnel shear deformation are 13.47 mm, 22.24 mm, and 16.37 mm. The results obtained using the method proposed in this study are closest to the measured values, and they are smaller than the results obtained when tunnel shear deformation is ignored, and approximates the findings in reference [15]. It can be seen from the curve obtained using the method proposed in this study that the tunnel beyond the excavation length of the foundation pit has produced a slight settlement. This is due to the drop in the water level outside the pit, which leads to an increase in the effective stress of the soil outside the pit and thus causes settlement of the tunnel. The same phenomenon also occurs in the engineering cases in literature[7, 20]. In summary, the accuracy and rationality of the method proposed in this study are proved.

**Fig. 7 Comparison with existing literature**

## 6 Parameters analysis

To examine the influencing factors of tunnel deformation caused by foundation pit excavation and dewatering, a basic model was established based on the engineering parameters in the numerical example verification for parameter analysis. The effects of foundation pit excavation length, width, depth, tunnel burial depth, dropdown, and tunnel–pit relative position on the deformation of the existing tunnel were mainly studied. The control variable method was used in the analysis process.

### 6.1 Excavation length of foundation pit

To study the influence of the excavation length of the foundation pit on the deformation of the existing tunnel, the excavation lengths were taken as 20, 25, 30, 35, 40, 45, and 50 m.

Figures 8 and 9 show the tunnel displacement curve and maximum displacement curve caused by foundation pit excavation and dewatering under different excavation lengths. It can be observed from Fig. 8 that the maximum uplift displacement of the tunnel occurs at the position  $x=0$  (located in the center of the foundation pit), and the uplift value gradually decreases toward both sides until settlement occurs near the edge of the foundation pit. This is attributed to the fact that dewatering causes the water level outside the pit to drop and the effective stress in the soil to increase. The force direction is opposite to the unloading direction of foundation pit excavation. As a result, the tunnel rises on the inside of the foundation pit and settles on the outside. In addition, as the excavation length increases, the maximum uplift of the tunnel gradually increases, and the settlement location gradually moves away from the center of the foundation pit. This can be explained that the increase in the excavation length of the foundation pit leads to an increase in the unloading amount of the soil and in scope of influence along the tunnel length direction. Figure 9 shows that when the excavation length increases from 20 m to 50 m, the maximum vertical displacement of the tunnel increases from 6.45 mm to 23.93 mm, and the increasing trend decreases slightly.

### 6.2 Excavation width of foundation pit

To examine the influence of the excavation width of the foundation pit on the deformation of the existing tunnel, the excavation widths were taken as 15, 20, 25, 30, 35, 40, 45, and 50 m. Figures 10 and 11 show the



tunnel displacement and maximum displacement caused by foundation pit excavation and dewatering under different excavation widths. Figure 10 shows that as the excavation width increases, the maximum values of tunnel uplift and settlement increase. The tunnel uplift value increases because the excavation unloading load increases with the excavation width. The reason for the increased settlement of the tunnel outside the pit is that the increase in excavation width raises the degree and scope of the impact of dewatering on the surrounding water level. Figure 11 illustrates that when the excavation width increases from 15 m to 50 m, the maximum vertical displacement of the tunnel gradually increases from 10.62 mm to 20.47 mm, and the increasing trend decreases significantly, and compared with the foundation pit excavation length changes, and the width changes have less impact on tunnel deformation.

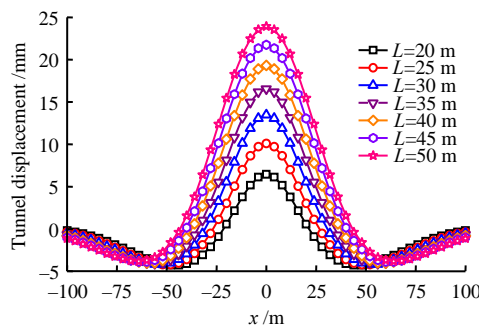


**Fig. 8** Curves of tunnel displacement under different lengths of excavation

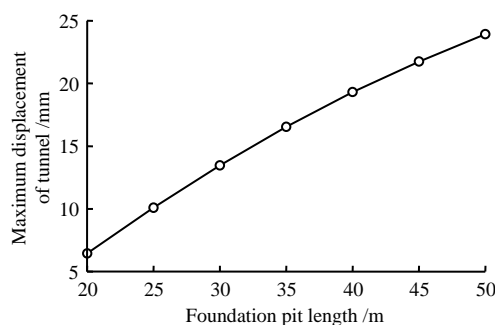


**Fig. 9** Maximum displacement curve under different lengths of excavation

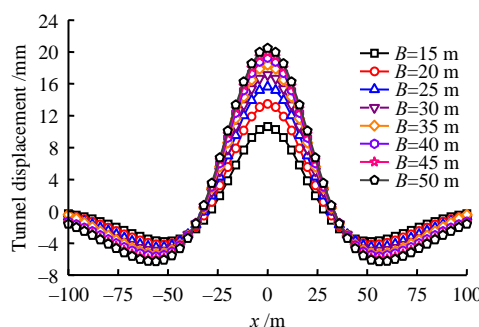


**Fig. 10** Curves of tunnel displacement under different widths of excavation

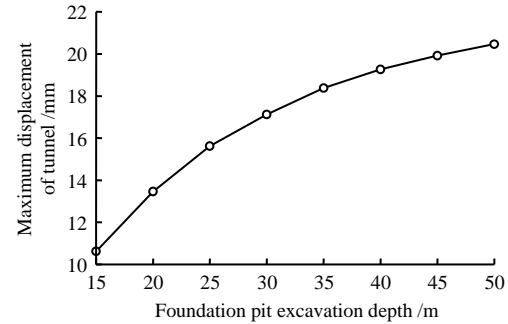


**Fig. 11** Maximum displacement curve under different widths of excavation

### 6.3 Tunnel burial depth

The tunnel burial depths of 2, 14, 16, 18, 20, 22, and 24 m were taken to investigate the influence of the tunnel burial depth on the deformation of the existing tunnel. Figures 12 and 13 show the tunnel displacement and maximum displacement caused by foundation pit excavation and dewatering under different tunnel burial depths. Figure 12 shows that the uplift of the tunnel gradually decreases as the tunnel depth increases. This is due to the fact that the deeper the tunnel is buried, the greater the net distance is between it and the excavation of the foundation pit, and the less affected by the unloading of the foundation pit excavation. It is evident from Figure 13 that when the tunnel burial depth increases from 12 m to 24 m, the maximum vertical displacement of the tunnel gradually decreases from 15.49 mm to 4.85 mm, and the change trend within this range is almost unchanged.

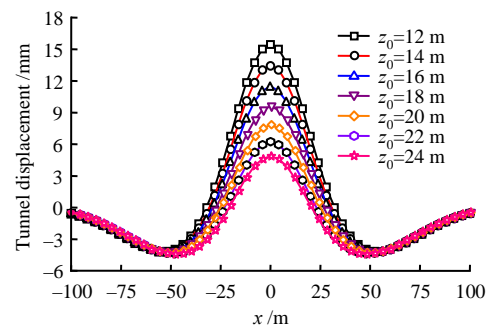


**Fig. 12** Curves of tunnel displacement under different burial depths of tunnel

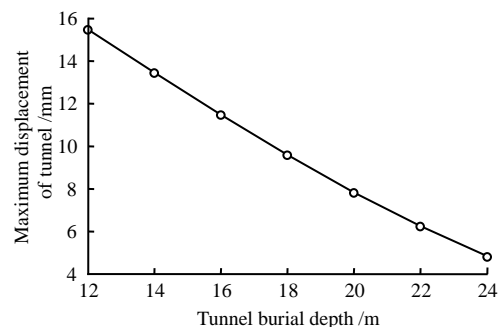


**Fig. 13** Maximum displacement curve under different burial depths of tunnel

#### 6.4 Excavation depth of foundation pit

To study the influence of foundation pit excavation depth on tunnel deformation, five excavation depths (6, 7, 8, 9, and 10 m) were selected for analysis. And the groundwater level is 1 m beneath the pit bottom for each excavation depth. Figures 14 and 15 show the tunnel displacement and maximum displacement caused by foundation pit excavation and dewatering under different excavation depths.

It can be observed from Fig.14 that as the excavation depth increases, the uplift and settlement of the tunnel increase. This is attributed to the fact that as the excavation depth of the foundation pit increases, the unloading effect of the soil on the tunnel increases, and the groundwater level in the pit also decreases with the increase of the excavation depth. Therefore, the additional stress caused by dewatering on the tunnel also increases. Figure 15 displays that when the excavation depth increases from 6 m to 10 m, the maximum vertical displacement of the tunnel gradually increases from 9.22 mm to 18.58 mm, and the change trend within this range almost remains unchanged.

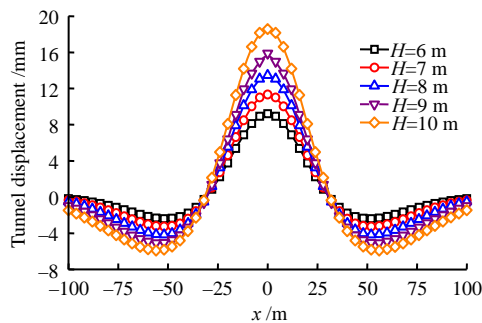


Fig. 14 Curves of tunnel displacement under different depths of excavation

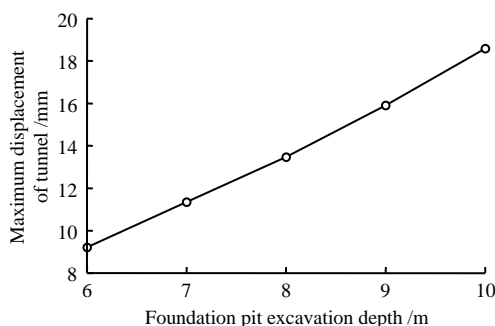


Fig. 15 Maximum displacement curve under different depths of excavation

#### 6.5 Drawdown

The influence of the drawdown on the tunnel deformation was analyzed selecting five drawdowns 8, 10, 12, 14, and 16 m. Figures 16 and 17 show the tunnel displacement and maximum displacement caused by foundation pit excavation and dewatering under different dropdowns. As shown in Fig.16, as the drawdown increases, the uplift of the tunnel gradually decreases, and the settlement gradually increases and

is gradually greater than the uplift. It should be noted that when the water level drops to 14 or 16 m, the water level has dropped below the tunnel axis. In Eq. (8),  $h_1$  is the distance from the tunnel axis to the bottom of the pit, that is, the additional stress caused by the drop in the water level in the pit remains unchanged. It can be observed from Fig.17 that when the drawdown increases from 8 m to 16 m, the maximum uplift of the tunnel decreases from 13.47 mm to 0.72 mm, and the maximum settlement increases from 4.17 mm to 11.58 mm, and the changing trends are somewhat weakened.

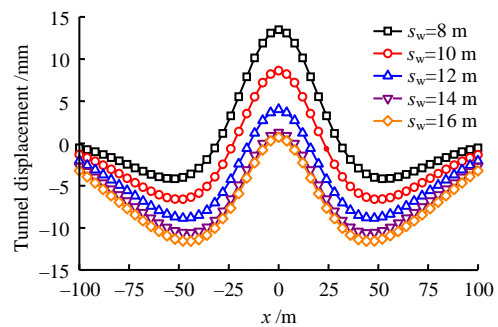


Fig. 16 Curves of tunnel displacement under different drawdowns

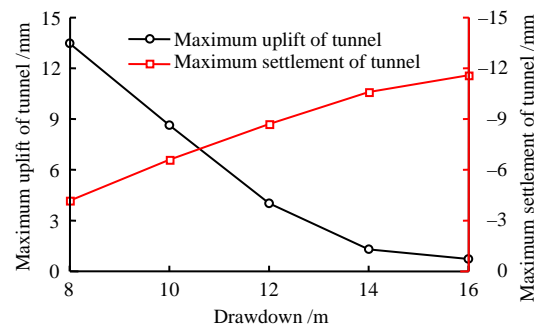


Fig. 17 Maximum displacement curves under different drawdowns

#### 6.6 Relative position of the foundation pit

To study the influence of the relative position of the foundation pit on tunnel deformation, eight tunnels at different positions were selected for analysis. The tunnel axis at each position is parallel to the length direction of the foundation pit, and only the distance  $d$  between the center of the foundation pit and the tunnel axis changes, and  $d$  is selected to be 0, 7, 14, 21, 28, 35, 42, and 49 m.

Figures 18 and 19 show the tunnel displacement and maximum displacement caused by foundation pit excavation and dewatering when the tunnel is in different positions. It can be seen from Figure 18 that as the distance between the tunnel axis and the center of the foundation pit increases, the main deformation of the tunnel changes from uplift to settlement. This is mainly caused by two reasons: (i) As the distance increases, the influence of foundation pit unloading on the tunnel gradually weakens, and the caused tunnel uplift decreases (ii) When the distance between the

tunnel axis and the center of the foundation pit is less than 10 m, the tunnel axis is located within the scope of foundation pit excavation, the soil removed from the foundation pit is not included in the additional stress caused by dewatering. When the distance is greater than 10 m, the soil layer above the tunnel axis has not been excavated, and the calculation of additional stress considers the effect of this part of the soil. Therefore, the additional stress caused by dewatering on the tunnel suddenly increases, and the main deformation of the tunnel becomes settlement. Hence, the effects of foundation pit excavation and dewatering on the tunnel directly below it and on its side may be completely different. From Fig.19, it is found that the displacement is the largest when the tunnel is located directly under the foundation pit. As the distance between the tunnel and the foundation pit increases, the maximum displacement of the tunnel first decreases in the uplift, then increases in the settlement value, and then the settlement value decreases again. According to the relative position of the foundation pit, the area where the tunnel is located is divided into an area with reduced uplift, an area with increased settlement, and an area with reduced settlement.

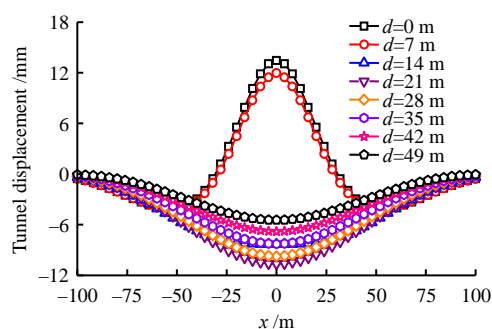


Fig. 18 Curves of tunnel displacement under different positions

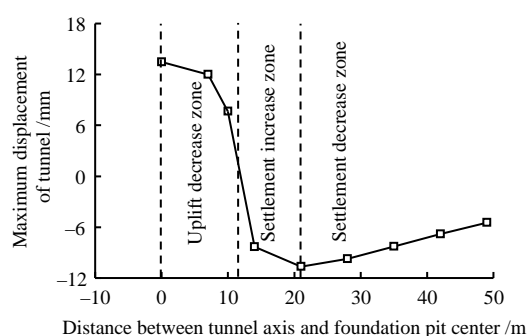


Fig. 19 Maximum displacement curve under different positions

## 7 Conclusions

This study presents a theoretical calculation method for the deformation of the underlying shield tunnel caused by the combined effects of excavation and dewatering. After a thorough analysis, the following main conclusions have been drawn:

(1) The additional stress in the tunnel caused by the unloading of the pit bottom and pit walls during foundation pit excavation and the increase in effective stress in the soil during dewatering is considered. The Pasternak-Timoshenko foundation beam model, which can consider the shear deformation of the tunnel and foundation soil, is used to simulate the interaction between the tunnel and the soil, and the analytical solution for the longitudinal deformation of the underlying shield tunnel is derived.

(2) The deformation monitoring data of the existing shield tunnel caused by foundation pit excavation and dewatering in actual projects were compared with the results calculated using the method in this study. It is found that the calculation results in this study, which consider the influence of dewatering and shear deformation of the tunnel, closely match the measured data, especially when compared to the results obtained by ignoring the influence of dewatering and neglecting the shear deformation of the tunnel.

(3) As the excavation length, width and depth of the foundation pit increase, the maximum uplift of the tunnel increases significantly. As the tunnel burial depth increases, the impact of foundation pit excavation on the tunnel weakens and the tunnel deformation decreases. As the drawdown increases, the tunnel uplift decreases and the settlement increases.

(4) Based on the relative positions of the tunnel and the foundation pit, the tunnel deformation can be categorized into three distinct areas: decreased uplift values, increased settlement values, and decreased settlement values, in that order, as the distance between the tunnel axis and the center of the pit increases. The largest tunnel displacement occurs when the tunnel is located directly under the foundation pit. Hence, it is advisable to avoid construction directly above the tunnel. Alternatively, it is recommended that excavation be carried out in zones from a farther distance to a nearer distance according to the tunnel's proximity.

It is important to note that in urban areas, foundation pit excavation projects often encounter numerous existing underground structures in their vicinity. Recent research<sup>[33]</sup> has indicated that these existing underground structures can lead to a greater drawdown, resulting in increased settlement. This research demonstrates that underground structures can impede the movement of soil surrounding the foundation pit, thereby reducing the displacement of retaining structures and soil deformation<sup>[33–34]</sup>. If a tunnel is located near an existing underground structure, its deformation is also likely to be reduced. However, since the impact of underground structures on groundwater levels and soil movements cannot be accurately determined, the method in this study does not consider the influence of underground structures surrounding the foundation pit. From a practical engineering perspective, further discussion is needed in this area. It should be clarified that the proposed method in this study can relatively quickly and

accurately predict the deformation of the tunnel below the excavation surface of the foundation pit. Nonetheless, the prediction of the deformation of the tunnel located on the side of the foundation pit and buried deeper than the excavation surface requires further study.

## References

- [1] DING Zhi, ZHANG Xiao, LIANG Fa-yun, et al. Research and prospects regarding the effect of foundation pit excavation on an adjacent existing tunnel in soft soil[J]. *China Journal of Highway and Transport*, 2021, 34(3): 21.
- [2] ZENG Chao-feng, BAI Ning, YUAN Zhi-cheng, et al. Effect of buried depth of adjacent structure on the foundation pit deformation during pre-excavation dewatering[J]. *Journal of China University of Mining & Technology*, 2022, 51(2): 283–292.
- [3] LIU Bo, ZHANG Ding-wen, LI Jian-chun. Prediction formula and its application of existing tunnel deformation induced by laterally adjacent deep excavation based on case statistics[J]. *Rock and Soil Mechanics*, 2022, 43(Suppl.1): 501–512.
- [4] ZENG Chao-feng, XUE Xiu-li, SONG Wei-wei, et al. Mechanism of foundation pit deformation caused by dewatering before soil excavation: an experimental study[J]. *Rock and Soil Mechanics*, 2020, 41(9): 2963–2972, 2983.
- [5] ZENG Chao-feng, SUN Hai-yu, XUE Xiu-li, et al. Responses of adjacent building pile foundation to dewatering in multi-aquifer system[J]. *China Civil Engineering Journal*, 2023, 56(8): 164–173, 183.
- [6] ZENG Chao-feng, WANG Shuo, SONG Wei-wei, et al. Control effect of cross walls on metro foundation pit deformation induced by pre-excavation dewatering in soft soils[J]. *Chinese Journal of Rock Mechanics and Engineering*, 2021, 40(6): 1277–1286.
- [7] BI Shu-qi, GAN Bin-lin, LIANG Ya-hua, et al. Measurement and analysis of the influence of foundation pit excavation on existing short distance tunnel[J]. *Science Technology and Engineering*, 2022, 22(3): 1198–1204.
- [8] WEN Suo-lin. Construction technology of deep open excavation above running metro tunnels[J]. *Chinese Journal of Geotechnical Engineering*, 2010, 32(Suppl.2): 451–454.
- [9] GUO Peng-fei, YANG Long-cai, ZHOU Shun-hua, et al. Measured data analysis of uplift deformation of underlying tunnel caused by foundation pit excavation[J]. *Rock and Soil Mechanics*, 2016, 37(Suppl.2): 613–621.
- [10] HE Zhong-ming, WANG Pan-pan, WANG Li-jun, et al. Influence of deep foundation pit construction on adjacent subway tunnel deformation and parameter sensitivity analysis[J]. *Journal of Chang'an University (Natural Science Edition)*, 2022, 42(4): 63–72.
- [11] ZHANG Zhi-guo, XU Chen, LIU Ming, et al. Deformation analysis of metro tunnel considering impacts of dewatering excavation in foundation pit engineering[J]. *Journal of China University of Mining & Technology*, 2015, 44 (2): 241–248.
- [12] OU Xue-feng, ZHANG Xue-min, LIU Xue-qin, et al. Analytic calculation method of underlying tunnel deformation caused by excavation and dewatering of upper pit[J]. *Journal of the China Railway Society*, 2019, (3): 8.
- [13] XU Chang-jie, ZENG Yi-ting, TIAN Wei, et al. Analytical analysis of the influence on adjacent pipelines induced by dewatering based on Pasternak model[J]. *Journal of Shanghai Jiaotong University*, 2021, 55(6): 11.
- [14] LIANG R, WU W, YU F, et al. Simplified method for evaluating shield tunnel deformation due to adjacent excavation[J]. *Tunnelling and Underground Space Technology*, 2018, 71(1): 94–105.
- [15] WANG Zu-xian, SHI Cheng-hua, GONG Chen-jie, et al. Analytical method to estimate the influence of foundation pit excavation adjacent to the station(working shaft) on the underlying shield tunnel[J]. *Rock and Soil Mechanics*, 2022, 43(8): 2176–2190.
- [16] LIANG R, KANG C, XIANG L, et al. Responses of in-service shield tunnel to overcrossing tunnelling in soft ground[J]. *Environmental Earth Sciences*, 2021, 80: 183.
- [17] ZHANG D M, HUANG Z K, LI Z L, et al. Analytical solution for the response of an existing tunnel to a new tunnel excavation underneath[J]. *Computers and Geotechnics*, 2019, 108(4): 197–211.
- [18] LIANG R, XIA T, HUANG M, et al. Simplified analytical method for evaluating the effects of adjacent excavation on shield tunnel considering the shearing effect[J]. *Computers & Geotechnics*, 2017, 81(1): 167–187.
- [19] ZHENG Gang, WANG Qi, DENG Xu, et al. Influence of pressure-relief of confined aquifer on existing tunnel under conditions of different inserted lengths of diaphragm wall[J]. *Rock and Soil Mechanics*, 2014, 35(Suppl.2): 412–421, 428.
- [20] ZHOU Shou-qiang, WANG Peng-cheng, WANG Jing. Analysis of the effect of dewatering excavation of deep foundation pit in phreatic aquifer on underlying tunnel[J]. *Journal of Hefei University of Technology (Natural Science)*, 2022, 45(3): 356–361.
- [21] MINDLIN RAYMOND D. Force at a point in the interior of a semi-infinite solid[J]. *Physics*, 1936, 7(5): 195–202.
- [22] ZENG Yi-ting. Study on the influence of foundation pit dewatering and excavation on surrounding pipelines[D].

- Hangzhou: Zhejiang University, 2020.
- [23] VERRUIJT A. Theory of groundwater flow[M]. [S. l.]: Macmillan Education UK, 1982.
- [24] SHEN S L, WU H N, CUI Y J, et al. Long-term settlement behaviour of metro tunnels in the soft deposits of Shanghai[J]. *Tunnelling and Under- ground Space Technology*, 2014, 40(2): 309–323.
- [25] WU H N, SHEN S L, LIAO S M, et al. Longitudinal structural modelling of shield tunnels considering shearing dislocation between segmental rings[J]. *Tunnelling and Underground Space Technology*, 2015, 50(8): 317–323.
- [26] KE Wen-hai, GUAN Ling-xiao, LIU Dong-hai, et al. Research on upper pipeline-soil interaction induced by shield tunnelling[J]. *Rock and Soil Mechanics*, 2020, 41(1): 221–228, 234.
- [27] ATTEWELL P B, YEATES J, SELBY A R. Soil movements induced by tunnelling and their effects on pipelines and structures[M]. London: Blackie and Son Ltd., 1986:128–132.
- [28] TANAHASHI H. Formulas for an infinitely long Bernoulli-Euler beam on the Pasternak model[J]. *Journal of the Japanese Geotechnical Society*, 2004, 44(5): 109–118.
- [29] XU Ling. Research of the longitudinal settlement of soft soil shield tunnel[D]. Shanghai: Tongji University, 2005.
- [30] ZHANG X, OU X, YANG J, et al. Deformation response of an existing tunnel to upper excavation of foundation pit and associated dewatering[J]. *International Journal of Geomechanics*, 2016, 17(4): 04016112.1–04016112.14.
- [31] WU H N, SHEN S L, LIAO S M, et al. Longitudinal structural modelling of shield tunnels considering shearing dislocation between segmental rings[J]. *Tunnelling and Underground Space Technology*, 2015, 50: 317–323.
- [32] SHIBO Y, YOSHIHIKO K, JAPANESE A, et al. The method of evaluating the rigidity of handicrafts in the long direction[C]//Collection of Papers of the Civil Society. Tokyo: Paper Editorial Committee of Civil Engineering Society, 1988: 319–327.
- [33] ZENG Chao-feng, ZHANG Zu-hao, GAO Wen-hua, et al. Barrier effect of surrounding group pile foundation on pit deformation induced by dewatering inside an excavation[J/OL]. *Chinese Journal of Geotechnical Engineering*[2023-10-25].<https://kns.cnki.net/kcms/detail/32.1124.TU.20220708.0948.002.html>.
- [34] XUE Xiu-li, LIAO Huan, ZENG Chao-feng, et al. Barrier effects of existing underground structures on deformation of strata induced by dewatering of foundation pits[J]. *Chinese Journal of Geotechnical Engineering*, 2023, 45(1): 103–111.